Original Paper

Brain, Behavior and Evolution

Brain Behav Evol 2003;61:28–44
DOI: 10.1159/000068879

Received: October 1, 2002
Returned for revision: November 11, 2002
Accepted after revision: November 26, 2002

Evolution of Specialized Pyramidal Neurons in Primate Visual and Motor Cortex

Chet C. Sherwood[a,b,c] Paula W.H. Lee[b] Claire-Bénédicte Rivara[b,d] Ralph L. Holloway[a,c] Emmanuel P.E. Gilissen[e,f] Robert M.T. Simmons[f] Atiya Hakeem[g] John M. Allman[g] Joseph M. Erwin[h] Patrick R. Hof[b,c,h]

[a]Department of Anthropology, Columbia University, New York, N.Y., [b]Kastor Neurobiology of Aging Laboratory and Fishberg Research Center for Neurobiology, Mount Sinai School of Medicine, New York, N.Y., [c]New York Consortium in Evolutionary Primatology, New York, N.Y., USA; [d]Department of Psychiatry (Neuropsychiatry Division), HUG Belle-Idée, University of Geneva School of Medicine, Geneva, Switzerland; [e]Institut Royal des Sciences Naturelles de Belgique, Département d'Anthropologie, Brussels, Belgium; [f]Department of Anatomical Sciences, Medical School, University of the Witwatersrand, Johannesburg, South Africa; [g]Division of Biology, California Institute of Technology, Pasadena, Calif., [h]Foundation for Comparative and Conservation Biology, Rockville, Md., USA

Key Words
Mammals · Primates · Brain evolution · Betz cell · Meynert cell · Motor cortex · Visual cortex

Abstract
The neocortex of primates contains several distinct neuron subtypes. Among these, Betz cells of primary motor cortex and Meynert cells of primary visual cortex are of particular interest for their potential role in specialized sensorimotor adaptations of primates. Betz cells are involved in setting muscle tone prior to fine motor output and Meynert cells participate in the processing of visual motion. We measured the soma volumes of Betz cells, Meynert cells, and adjacent infragranular pyramidal neurons in 23 species of primate and two species of non-primate mammal *(Tupaia glis* and *Pteropus poliocephalus)* using unbiased stereological techniques to examine their allometric scaling relationships and socioecological correlations. Results show that Betz somata become proportionally larger with increases in body weight, brain weight, and encephalization whereas Meynert somata remain a constant proportion larger than other visual pyramidal cells. Phylogenetic variance in the volumetric scaling of these neuronal subtypes might be related to species-specific adaptations. Enlargement of Meynert cells in terrestrial anthropoids living in open habitats, for example, might serve as an anatomical substrate for predator detection. Modification of the connectional and physiological properties of these neurons could constitute an important evolutionary mode for species-specific adaptation.

Introduction

During primate evolution the neocortex has undergone expansion, addition of areas, and the elaboration of novel neuronal subtypes leading to great diversity in sensorimo-

KARGER

Fax + 41 61 306 12 34
E-Mail karger@karger.ch
www.karger.com

Accessible online at:
www.karger.com/bbe

Patrick R. Hof
Kastor Neurobiology of Aging Laboratories
Mount Sinai School of Medicine, Box 1639
One Gustave L. Levy Place, New York, NY 10029 (USA)
Tel. +1 212 659 5904, Fax +1 212 849 2510, E-Mail patrick.hof@mssm.edu

tor and cognitive specializations [Holloway, 1996; Allman, 1999; Nimchinsky et al., 1999]. Among the neuronal subtypes found in primate neocortex, Betz cells of primary motor cortex (Brodmann's area 4) and Meynert cells of primary visual cortex (Brodmann's area 17) have attracted particular attention due to their large cellular volume concomitant with unique dendritic arborization patterns, distinctive connections, thick myelinated axons, and intense immunostaining for nonphosphorylated neurofilament protein [Chan-Palay et al., 1974; Scheibel and Scheibel, 1978; Meyer, 1987; Hof and Morrison, 1995; Hof et al., 2000; Kaas, 2000]. Although comparable neurons have been described in other mammals, their exceptionally large size in primates [Le Gros Clark, 1942; Zilles, 1990; Kaas, 2000], for whom dexterous digital movement and vision are important [Le Gros Clark, 1959; Martin, 1990], suggests that these neuronal subtypes constitute cellular substrates for specialized sensorimotor capacities.

The giant cells of Betz [Betz, 1874, 1881; Brodmann, 1903, 1909; von Economo and Koskinas, 1925; Vogt and Vogt, 1942] are a prominent feature of area 4, found either in isolation or in small groups of three to four cells in the lower half of layer V [Brodmann, 1909; von Economo and Koskinas, 1925; von Bonin, 1949; Meyer, 1987]. In contrast to other layer V pyramidal cells, which have a single apical dendritic shaft and dendritic arbors that exit the soma from basal angles, Betz cells possess a greater number of primary dendritic shafts that leave the soma asymmetrically at almost any point around its surface [Braak and Braak, 1976; Scheibel et al., 1977; Scheibel and Scheibel, 1978; Meyer, 1987]. Although these dendrites project into all cortical layers, most horizontal dendritic arbors occupy layers V and VI with some reaching into the white matter [Meyer, 1987]. In the generation of movement, Betz cells provide phasic early output that prepares flexor muscle tone prior to the recruitment of smaller surrounding pyramidal neurons that fine tune the specific motor program [Evarts, 1965; Scheibel and Scheibel, 1978]. In humans, Betz cells are largest and most numerous in the cortical representation of the leg, where axons project farther along the corticospinal tract to reach large masses of antigravity muscles [Lassek, 1948]. In contrast, the volumes of other layer V pyramidal cells are homogeneous across the somatotopic representation [von Bonin, 1949; Zilles, 1990; Rivara et al., 2003].

Meynert cells [Meynert, 1867] constitute a second morphologically distinct subtype of pyramidal neuron in the primate neocortex [Chan-Palay et al., 1974; Palay, 1978]. They are located at the boundary between layers V and VI of area 17, occurring in small clusters in the calcarine representation of the far peripheral visual field and more solitarily in the opercular region [Hof et al., 2000]. Their thick axons ramify with collaterals projecting to both area MT/V5 and the superior colliculus [Spatz, 1975; Fries and Distel, 1983; Fries et al., 1985; Rockland and Knutson, 2001]. Based on this connectivity, Meynert cells are thought to be involved in the detection of motion in the visual field [Fries et al., 1985; Movshon and Newsome, 1996; Livingstone, 1998]. The basal dendrites and axon collaterals of Meynert cells extend horizontally to remote sites in layers V and VI providing an anatomic substrate for the integration of information and facilitation of responses across widespread areas of visual space [Le Gros Clark, 1942; Lund et al., 1975; Fries and Distel, 1983; Winfield et al., 1983; Rockland and Knutson, 2001]. Here we examine the properties of these specialized pyramidal cells with respect to brain and body size, as well as socioecological variables, to assess their allometric scaling and possible role in primate adaptations.

Materials and Methods

Specimens and Tissue Preparation

Samples of areas 4 and 17 were obtained from 41 adult individuals representing 23 primate and 2 non-primate mammalian species *(Tupaia glis* and *Pteropus poliocephalus)*. Between 1 and 5 individuals were available for analysis from each species (table 1). Most specimens were obtained postmortem or from terminally ill animals sacrificed for humane reasons and were fixed by immersion in 10% neutral formalin. Specimens of flying fox, macaque, patas, baboon, owl, and tamarin monkeys were obtained from animals perfused transcardially with 4% paraformaldehyde in the context of unrelated experiments. Great ape brains came from young and adult individuals (10–37 years old). Human brain specimens were obtained at autopsy from three neurologically normal individuals (69–85 years old) and were prepared as described previously [Rivara et al., 2003]. Samples were dissected from the lateral precentral gyrus or the lateral convexity of the cortex corresponding to the approximate location of forelimb representation of area 4. Intracortical microstimulation-based maps do not exist for many of the species included in the present study. Therefore, we estimated the location of forelimb representation by reference to written descriptions and illustrations published in mapping studies of motor cortex of the flying fox [Krubitzer et al., 1998], galago [Fogassi et al., 1994; Wu et al., 2000], marmoset [Krubitzer and Kaas, 1990], owl monkey [Gould et al., 1986; Preuss et al., 1996], squirrel monkey [Strick and Preston, 1978, 1982; Donoghue et al., 1992; Flaherty and Graybiel, 1995], macaque [Kwan et al., 1978; Humphrey, 1986; Sato and Tanji, 1989; Park et al., 2001], baboon [Craggs et al., 1976; Samulack et al., 1990; Waters et al., 1990], orang-utan [Leyton and Sherrington, 1917], gorilla [Leyton and Sherrington, 1917], chimpanzee [Grünbaum and Sherrington, 1903–04; Leyton and Sherrington, 1917; Hines, 1940; Dusser de Barenne et al., 1941; von Bonin, 1950], and human [Penfield and Boldrey, 1937; Yousri et al., 1997; Boroojerdi et al., 1999; Hlustik, 2001]. A second block was dissected from the occipital cortex includ-

ing area 17. Area 17 was identified on the basis of its location and distinct cytoarchitectural pattern [Allman and Kaas, 1971; Kaas et al., 1972; Newsome and Allman, 1980; Zilles et al., 1982; Kretz et al., 1986; DeBruyn et al., 1993; Preuss et al., 1993, 1999; Rosa et al., 1993, 1997; Zeki, 1993]. Every attempt was made to sample tissue consistently from only the right hemisphere. In the available materials, however, this could only be ensured for the anthropoids in the sample. Nonetheless, in light of evidence that neuronal sizes in area 4 [Hayes and Lewis, 1995] and area 17 [Galaburda et al., 2002] of normal humans do not exhibit hemispheric lateralization it is assumed that variation in our measurements due to hemisphere of origin is significantly smaller than variation due to interspecific differences. Each sample was sectioned at 50 μm perpendicular to the pial surface using a cryostat. From each specimen, a 1:15 series (non-human) or 1:50 series (human) of sections was immediately Nissl-stained with cresyl violet. In addition, three specimens *(Lagothrix, Alouatta,* and *Daubentonia)* from the Stephan comparative brain collection [Stephan et al., 1981, 1988] were included in this study.

Stereological Methods

Betz and Meynert cell were distinguished from neighboring pyramidal cells according to their laminar position and cytomorphologic features [Meynert, 1867; Ramón y Cajal, 1899; Tigges et al., 1981]. Betz cells are located preferentially in layer Vb of area 4 [von Economo and Koskinas, 1925] and are recognized in Nissl-stained material as large pyramidal neurons displaying a conspicuous nucleolus, a prominent rough endoplasmic reticulum, large lipofuscin deposits in the cell body, and dendritic branches leaving from the entire circumference of the soma [Campbell, 1905; Brodmann, 1909; Walshe, 1942; Braak and Braak, 1976; Scheibel and Scheibel, 1978; fig. 1, 2]. Meynert cells are located at the border between layers V and VI throughout area 17 where they form small aggregates of up to five neurons. In Nissl preparations Meynert cells are distinguished by their large soma size, squat shape, and often eccentrically positioned nucleus [Winfield et al., 1981; Fries, 1986; Hof et al., 2000; fig. 1, 2].

The volumes of Meynert somata, Betz somata, and neighboring pyramidal cell somata were estimated using a computer-assisted stereological software system consisting of a Zeiss Axiophot microscope equipped with a Zeiss MSP65 computer-controlled motorized stage, a Zeiss ZVS-47E video camera, a Macintosh G3 microcomputer, and NeuroZoom morphometry and stereology software [Nimchinsky et al., 2000]. Cellular volume measurements of specimens from the Stephan collection were conducted using a comparable stereology system at the Vogt Institut für Hirnforschung, Heinrich-Heine-Universität consisting of a Nikon Eclipse microscope and StereoInvestigator software (MicroBrightField Inc., Wiliston, VT). Identical stereological sampling techniques were used to quantify soma volumes across all specimens. From each specimen, two sections approximately 2.5 to 3.0 mm apart were sampled from visual and motor cortices. The boundaries of layer V (motor cortex) or layers V-VI (visual cortex) were outlined at low magnification (5×). After outlining the boundaries of the field of interest on the computer graphic display of each

Table 1. Sample data used in analyses

Taxon	n	Motor pyramid			Betz cell			Visual pyramid			Meynert cell		
		mean	SD	CV, %	mean	SD	CV, %	mean	SD	CV, %	mean	SD	CV, %
Pteropus poliocephalus	1	1,170	567	48	3,704	882	24	1,186	379	32	2,507	938	37
Tupaia glis	2	1,906	70	4	3,008	120	4	1,050	45	4	2,024	68	3
Loris tardigradus	1	851	246	29	1,756	608	35	654	266	41	1,409	511	36
Perodicticus potto	2	3,492	155	4	13,033	837	6	1,802	65	4	4,356	199	5
Galago senegalensis	1	1,488	58	4	3,052	267	9	–	–	–	–	–	–
Otolemur crassicaudatus	3	1,998	103	5	3,156	208	7	933	37	4	2,267	208	9
Lemur catta	2	2,584	159	6	9,457	680	7	1,590	53	3	2,713	89	3
Hapalemur griseus	1	1,748	720	41	3,440	1,656	48	784	292	37	1,890	1,032	55
Propithecus verreauxi	1	2,524	1,062	42	6,348	3,393	53	1,286	463	36	2,872	1,378	48
Daubentonia madagascariensis	1	1,979	1,187	60	6,127	2,082	34	1,143	232	20	3,602	1,601	44
Tarsius syrichta	1	1,457	120	8	3,927	300	8	815	41	5	1,826	103	6
Saguinus mystax	1	3,258	1,582	49	7,939	3,243	41	1,217	385	32	3,322	1,750	53
Aotus trivirgatus	2	3,561	132	4	9,644	642	7	1,156	40	3	3,331	179	5
Alouatta seniculus	1	5,541	2,055	37	26,361	9,242	35	1,007	257	26	3,070	1,060	35
Lagothrix lagotricha	1	2,096	950	45	5,869	1,846	31	1,236	387	31	2,617	1,306	50
Macaca fascicularis	2	4,079	232	6	14,530	1,266	9	1,249	55	4	3,321	206	6
Macaca fuscata	1	3,953	1,446	37	16,871	1,703	10	–	–	–	–	–	–
Macaca nigra	1	5,260	2,174	41	28,114	16,183	58	–	–	–	–	–	–
Papio cynocephalus	1	2,316	1,126	49	18,672	8,230	44	1,336	458	34	5,483	2,829	52
Papio anubis	1	4,166	1,676	40	28,732	15,525	54	945	333	35	4,597	1,763	38
Erythrocebus patas	2	2,603	872	33	23,062	11,799	51	1,484	401	27	8,611	4,994	58
Pongo pygmaeus	1	4,928	235	5	32,092	2,340	7	2,134	78	4	4,134	242	6
Gorilla gorilla	4	5,597	292	5	46,839	3,682	8	1,824	716	39	5,436	1,917	35
Pan troglodytes	5	4,559	254	6	32,022	2,346	7	1,718	605	35	6,498	3,062	47
Homo sapiens	1	5,031	2,174	43	55,125	29,225	53	2,168	77	4	6,159	423	7

Data come from the reference indicated in category heading unless otherwise noted.
[1] Stephan et al. [1981]; [2] Baron et al. [1996]; [3] Zilles and Rehkämper [1988]; [4] Harvey et al. [1987]; [5] personal observation (n = 2); [6] Fleagle [1999]; [7] Rowe [1996]; [8] Groves [2001]; [9] Clutton-Brock and Harvey [1980]; [10] Dunbar [1992]; [11] Heffner and Masterton [1983].

section, the software placed a set of optical disector frames (30 × 30 μm for non-hominoids; 100 × 100 μm for hominoids) in a systematic-random fashion corresponding to 5–10% of the outlined area. For each specimen the disector thickness was consistently set at 6 μm allowing for a minimum 2 μm guard zone on either side of the section. Using this systematic-random sampling design, Meynert somata, Betz somata, and surrounding pyramidal cell somata volumes were measured using the planar rotator technique with a vertical design [Vedel-Jensen and Gundersen, 1993] at high magnification with a 100 × Plan Neofluar/1.4 N.A. objective and Koehler illumination. Although our sections were not prepared isotropic-uniform-random, rotator analysis of cortical neurons has been shown to yield comparable results in coronal sections and isotropic-uniform-random sections [Schmitz et al., 1999] and, due to the orientation of the tissue in our preparations, not all neurons were necessarily cut along the same axis thereby allowing for a certain degree of randomness in the sample. Only neurons whose nucleus was enclosed within the counting frame or in contact with its permitted edges were analyzed, and the nucleolus was consistently chosen as a reference landmark for the focal plane during rotator analysis.

Statistical Analyses

For each sample, mean neuronal subtype volume, standard deviation, and coefficient of variation (CV) were calculated (table 1). On average, 225 neurons in each region of interest were sampled in each individual. The mean volume of non-specialized infragranular pyramidal cell somata was used to standardize specialized pyramidal cell data. As the principal source of output for cortical modules, infragranular pyramidal neuron soma volume is expected to be correlated with cortical module size [Mountcastle, 1998]. A Betz or Meynert ratio (mean specialized pyramidal cell soma volume/mean neighboring pyramidal cell soma volume) was calculated for each individual cortical region. This ratio is a shrinkage-independent variable that allows for comparisons of relative Betz and Meynert cell soma volumes across samples prepared using different histological techniques. For species where more than one individual was available, individual Betz and Meynert ratios were averaged to obtain a species mean value. These ratios were log-transformed to reduce skewness of the distributions while preserving proportionality of the ratios across the entire range of values [Smith, 1999].

Data from the literature were collected for species mean brain weight, body weight, and neocortex volume [Stephan et al., 1981; Harvey et al., 1987; Zilles and Rehkämper, 1988; Rowe, 1996; Fleagle, 1999; Groves, 2001]. When separate mean brain and body weight values for males and females were available, they were averaged to obtain a species mean. In addition, an Encephalization Quotient (EQ) was determined for each species by taking the ratio of actual over expected brain weight. Expected brain weights were calculated from species mean body weights by using Martin's [1981] formula relating brain and body weights in a sample of 309 placental mammals.

$$\log_{10} \text{brain wt.} = 0.755\ (\log_{10} \text{body wt.}) + 1.774$$

Neocortex vol[1]	Brain weight[4]	Body weight[6]	EQ	Dietary category[9]	Habitat category[9]	Group size[7]	Dexterity index[11]
2,710[2]	7.2[2]	695[2]	0.87	–	–	–	–
1,036	3.2[1]	170[1]	1.11	–	–	–	3
3,524	6.6[1]	322[1]	1.42	IN	ARB	4	–
6,683	14.3	833	1.50	FR	ARB	2	–
2,139	4.8[1]	213	1.41	FR	ARB	–	5
4,723	11.8	1,150	0.97	FR	ARB	6	5
–	25.6	2,210	1.29	FR	TER	17	5
–	14.7	916[7]	1.44	FO	ARB	6	–
13,170	26.7[1]	3,480[8]	0.95	FO	ARB	12	–
22,127	45.2[1]	2,800[1]	1.90	IN	ARB	2	–
1,768	4.0	111	1.93	IN[7]	ARB[7]	2	4
–	10.1[5]	525	1.50	–	ARB[7]	5.3[10]	–
9,950	18.2	775	2.02	FR	ARB	3.8[10]	–
31,660	52.0[1]	6,400[1]	1.17	FO	ARB	8.2[10]	–
65,873	101.0[1]	5,200[1]	2.66	FR	ARB	23.4[10]	5
–	69.2	4,475	2.04	FR	ARB	48	–
–	109.1	9,515	1.82	FR	TER	40	–
–	94.9	7,680	1.86	FR[7]	ARB[7]	47	–
–	169.1	17,050	1.82	FR	TER	28	6
140,142	175.1	19,200	1.72	FR	TER	51.2[10]	6
77,141	106.6	8,185	1.99	FR	TER	28.1[10]	–
219,800[3]	413.3	56,750	1.79	FR	ARB	3	6
341,444	505.9	120,950	1.24	FO	TER	7[10]	–
291,592	405.0[1]	52,750	1.85	FR	TER	53.5[10]	–
1,006,525	1,250	60,000	5.19	–	TER[7]	–	7

IN = Insectivorous; FR = frugivorous; FO = folivorous; ARB = arboreal; TER = terrestrial.

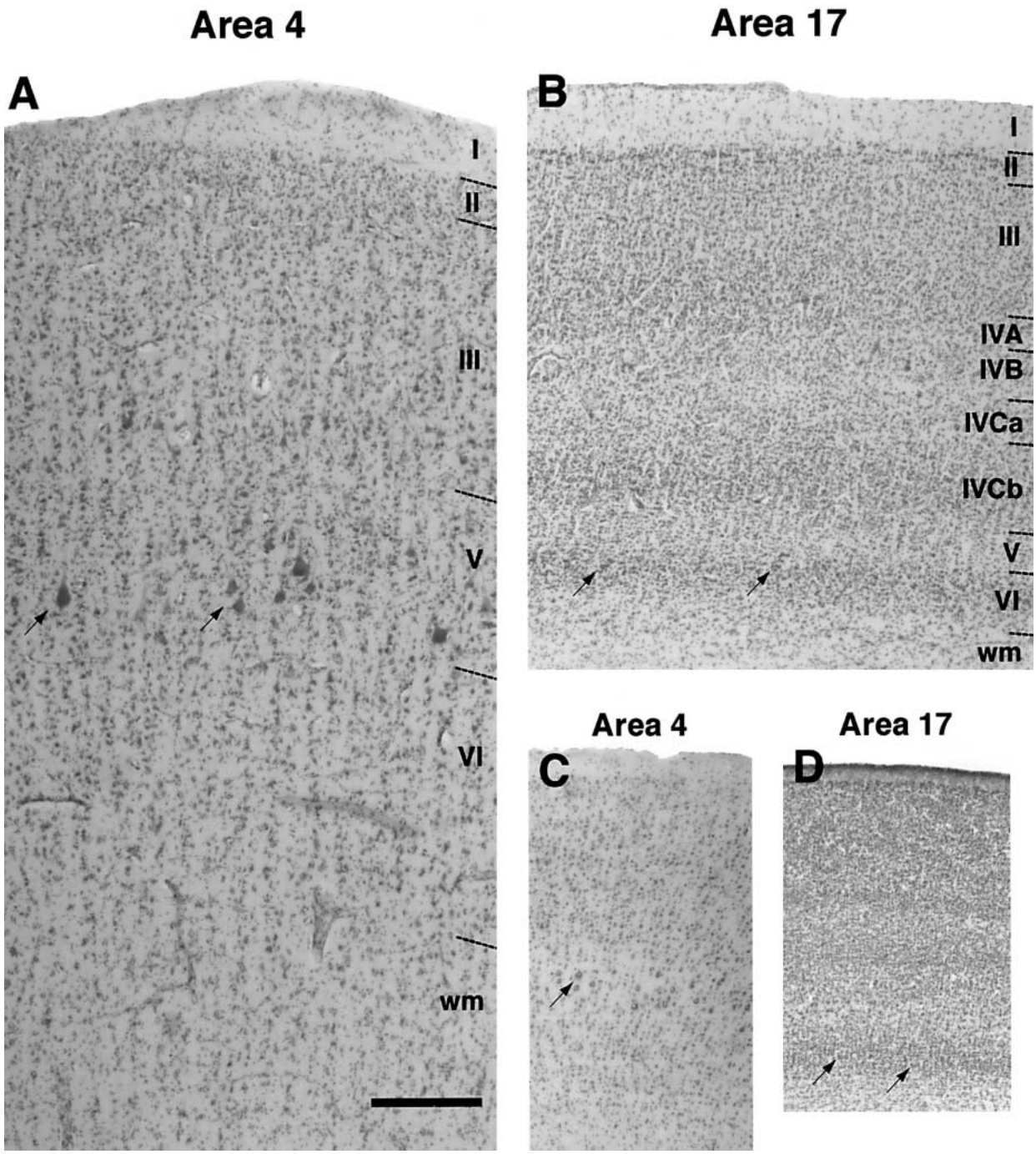

Fig. 1. Representative examples of the cytoarchitecture of primary motor cortex (area 4) and primary visual cortex (area 17) illustrating the laminar position of Betz and Meynert cells. Panels A and B are from the brain of *Pongo pygmaeus*. Note the thickness of area 4 (A) and the typical laminar pattern of area 17 (B). Area 17 is characterized by a granular appearance that contrasts with the prominent pyramidal neurons of the motor cortex. Relatively smaller neurons are seen in area 4 of *Lemur catta* (C). Area 17 of *Tarsius syrichta* (D), although much thinner, shows the same laminar pattern as that of *Pongo*. Betz cells are located preferentially in layer Vb of area 4 (arrows in A and C). Meynert cells are located at the border between layers V and VI throughout area 17 where they form small aggregates of up to five neurons (arrows in B). Scale bar (on A) = 150 μm (for A–D).

Data from the literature on maximum social group size found under natural circumstances, dietary category (i.e., insectivore, folivore, or frugivore), and habitat (i.e., arboreal or terrestrial) were used to explore socioecological correlations in the primate sample [Clutton-Brock and Harvey, 1980; Dunbar, 1992; Rowe, 1996].

All variables were first tested for normality using the Shapiro-Wilk W test, then log-transformed as necessary to meet assumptions of normality in subsequent analyses. For each individual cortical region, specialized pyramidal neurons were compared to neighboring pyramidal neurons using independent samples t-tests. The relationship between Betz and Meynert ratios and brain or body variables was explored using Pearson product moment correlation and one-way analysis of variance (ANOVA) was used to investigate socioecological relationships. Allometric scaling was examined using least-squares (LS) and reduced major-axis (RMA) regression of log-transformed data. For allometric analyses RMA might be preferred because, unlike LS regression, it does not assume that the independent variable is measured without error. Because estimates of slope obtained by RMA were contained within the 95% confidence intervals of the LS model for all regressions, only LS best-fit lines are shown in figures. Statistical significance was set at $p < 0.05$.

Results

Neurons that expressed the morphological and positional characteristics of Betz and Meynert cells were observed in all species examined, including relatively small-brained non-primate mammals and prosimians (fig. 2). Variability in soma volume was high for all neuronal subtypes as reflected by a mean CV of 26 ± 19%. Coefficient of variation was not correlated with brain weight for any neuron subtype. Volumes of Betz and Meynert somata were significantly larger than neighboring pyramidal cell somata in every species ($p < 0.05$). Thus, Betz and Meynert cells constitute distinctive neuronal populations based upon soma volume as well as cytomorphological features.

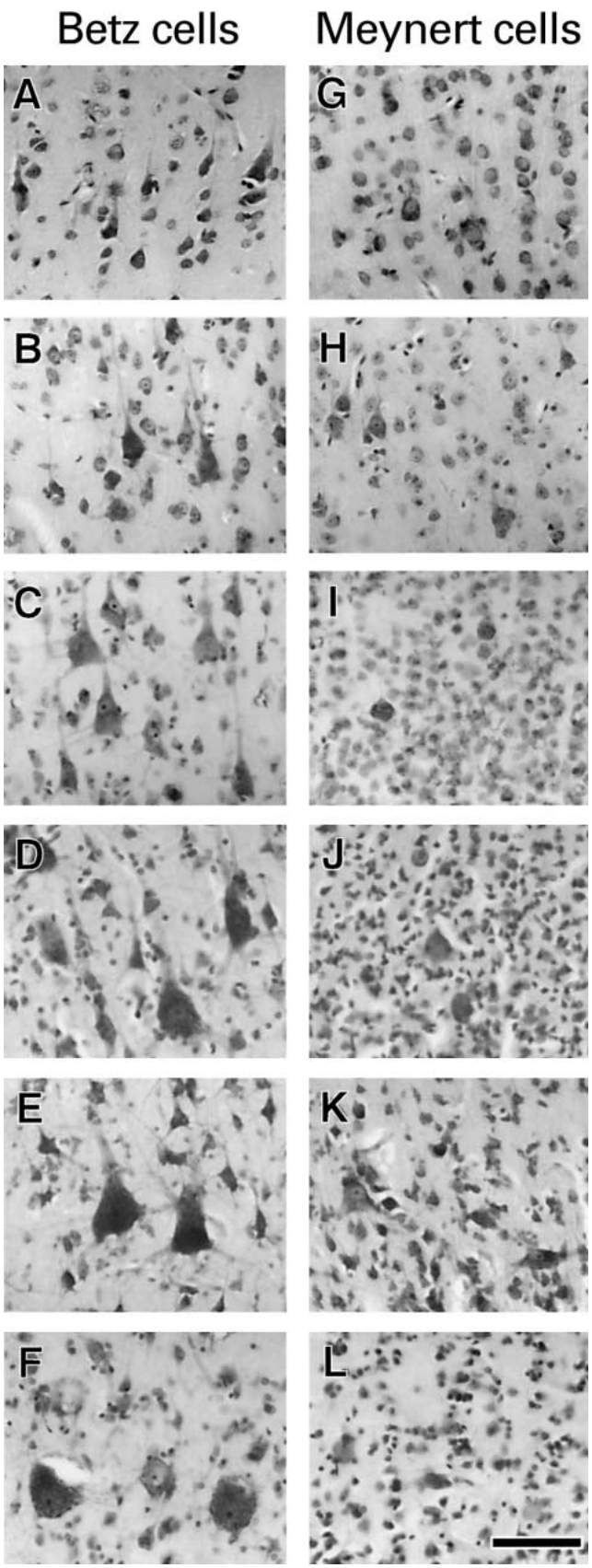

Fig. 2. Examples of Betz cells and Meynert cells illustrating their cytomorphologic characteristics. Betz cells (A–F) and Meynert cells (G–L) in *Perodicticus potto* (A and G), *Lemur catta* (B and H), *Aotus trivirgatus* (C and I), *Papio anubis* (D and J), *Gorilla gorilla* (E and K), and *Homo sapiens* (F and L). Betz cells are recognized as large pyramidal neurons displaying a conspicuous nucleolus, a prominent rough endoplasmic reticulum, large lipofuscin deposits in the cell body, and dendritic branches leaving from the entire surface of the soma. In Nissl preparations, Meynert cells are distinguished by their large soma size, squat shape, and often eccentrically positioned nucleus. Scale bar = 50 μm.

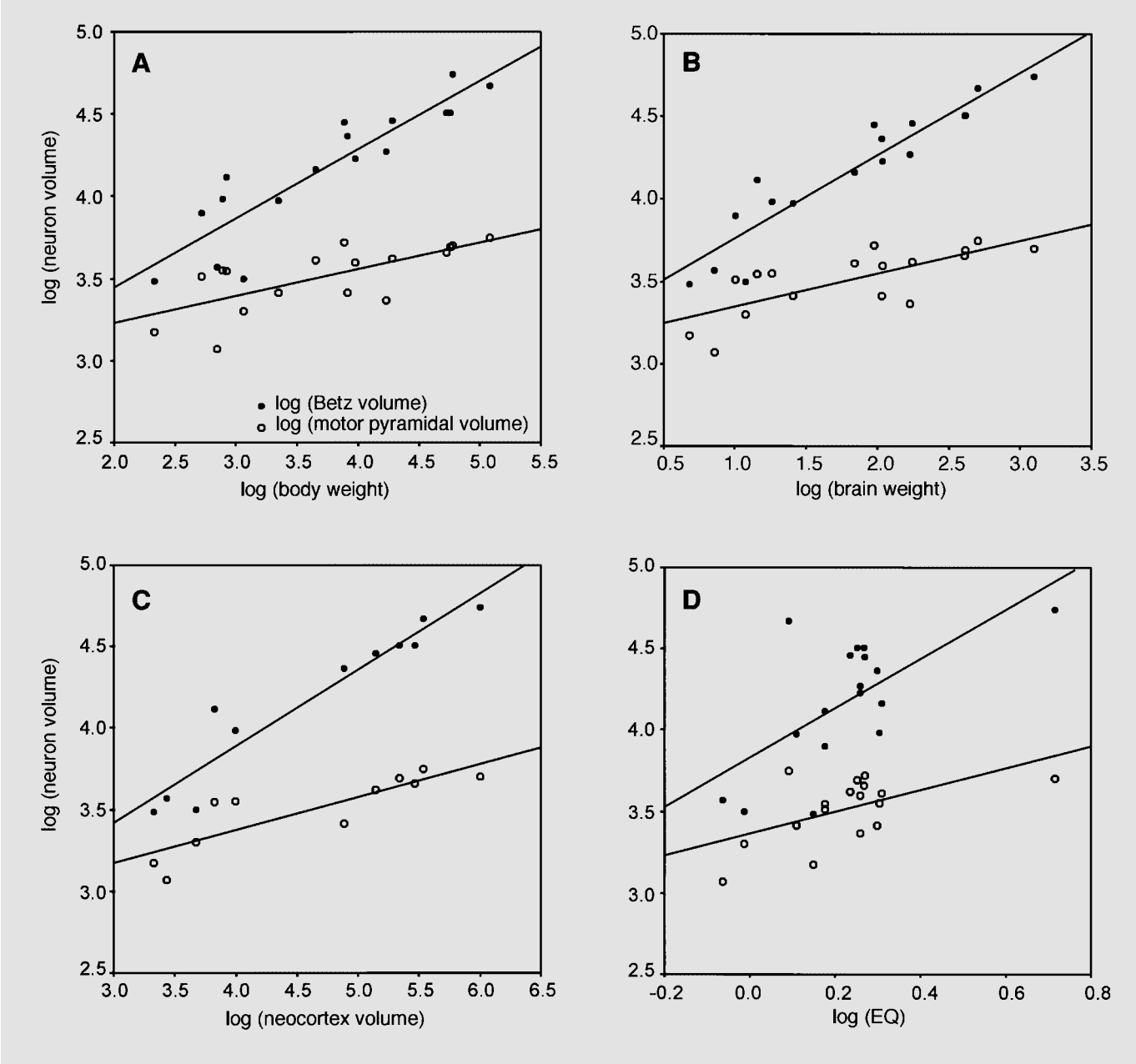

Fig. 3. Least-squares regression plots of infragranular pyramidal cell volumes in primary motor cortex. Cellular volumes are regressed against body weight (A), brain weight (B), neocortex volume (C), and EQ (D). Note that the regression slope is significantly steeper for Betz cells compared to other layer V motor pyramidal neurons. Regressions of cellular volumes against body weight, brain weight, and neocortex volume fit a linear relationship better than when regressed against EQ.

The tissue examined in the present study was not prepared using uniform histological techniques and absolute cellular volumes may be affected to different degrees by shrinkage artifact. To avoid this confound, scaling relationships of motor and visual pyramidal cells were first analyzed in a subset of the sample which was prepared using similar fixation and specimen preparation conditions. This subset included representative non-primate, prosimian, and anthropoid species (i.e., all species from table 1 except *Tupia glis*, *Loris tardigradus*, *Hapalemur*

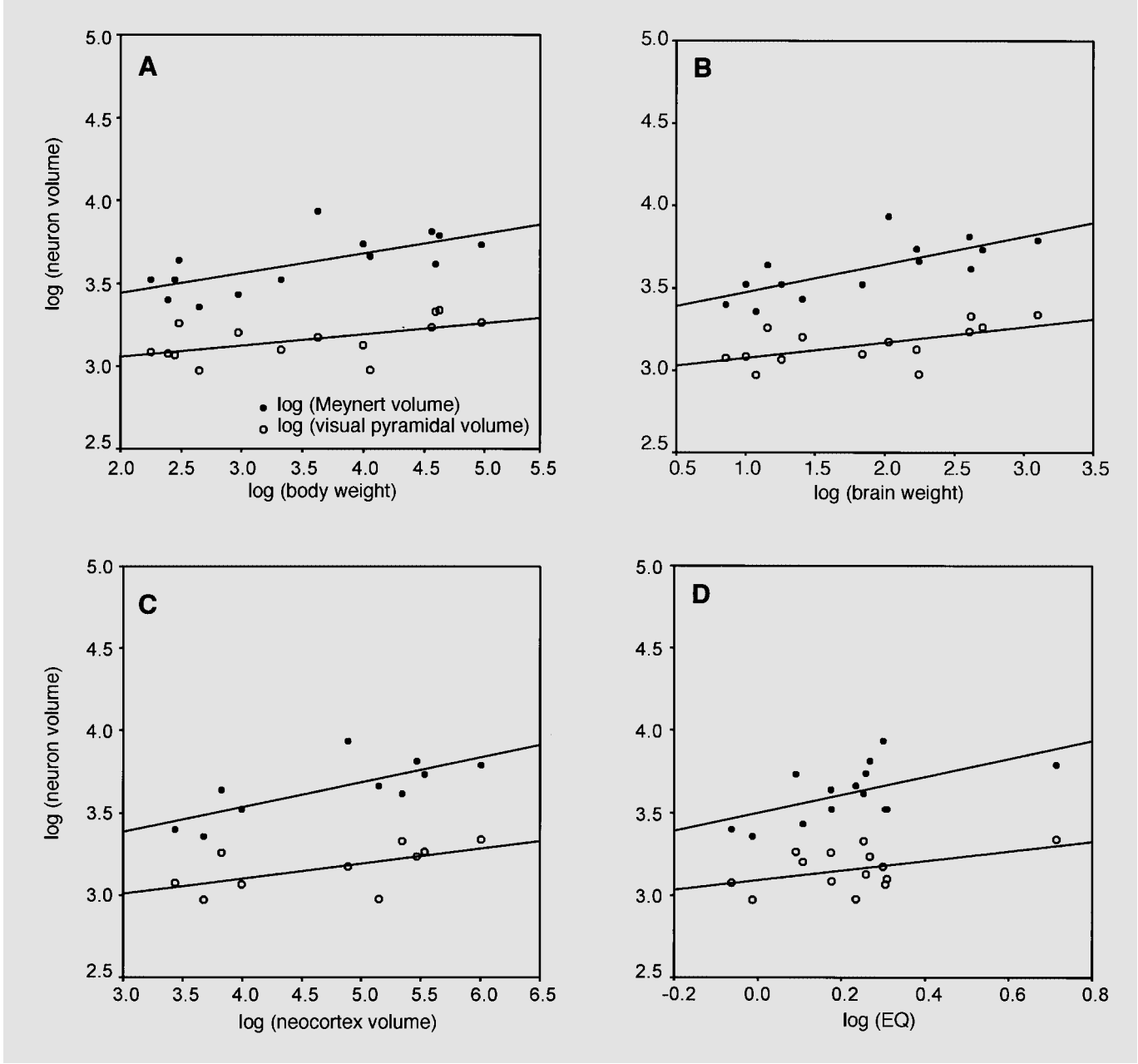

Fig. 4. Least-squares regression plots of infragranular pyramidal cell volumes in primary visual cortex. Cellular volumes are regressed against body weight (A), brain weight (B), neocortex volume (C), and EQ (D). Note that the regression slopes are similar for both subtypes of infragranular visual pyramidal neuron. As in the motor cortex (fig. 3) regressions of cellular volumes against body weight, brain weight, and neocortex volume fit a linear relationship better than EQ.

griseus, *Propithecus verreauxi*, *Daubentonia madagascariensis*, *Tarsius syrichta*, *Alouatta seniculus*, and *Lagothrix lagotricha*). The double-logarithmic regression of cell soma volumes showed that all neuronal subtypes have regression slopes that are less than 1, indicating that they scale with negative allometry with respect to brain and body size variables (fig. 3, 4; table 2). Comparison of coefficients of determination showed that soma volumes of all neuronal subtypes were predicted better by brain weight and neocortex volume than by body weight and EQ. Also,

Table 2. Regression statistics for allometric scaling of infragranular pyramidal neurons

	LS slope	LS confidence intervals	RMA slope	R^2	n
Motor pyramid					
Body weight	0.16	0.07–0.26	0.11	0.49	16
Brain weight	0.20	0.11–0.28	0.15	0.58	16
Neocortex volume	0.20	0.11–0.30	0.17	0.72	12
EQ	0.67	0.14–1.20	0.38	0.32	16
Betz cell					
Body weight	0.42	0.31–0.53	0.38	0.81	16
Brain weight	0.51	0.41–0.60	0.48	0.90	16
Neocortex volume	0.47	0.36–0.58	0.45	0.91	12
EQ	1.52	0.54–2.50	0.99	0.42	16
Visual pyramid					
Body weight	0.08	0.01–0.15	0.04	0.31	14
Brain weight	0.10	0.03–0.17	0.06	0.41	14
Neocortex volume	0.09	–0.01–0.19	0.06	0.36	11
EQ	0.30	–0.07–0.66	0.14	0.21	14
Meynert cell					
Body weight	0.14	0.05–0.23	0.10	0.47	14
Brain weight	0.18	0.10–0.27	0.13	0.62	14
Neocortex volume	0.15	0.04–0.26	0.11	0.57	11
EQ	0.55	0.08–1.02	0.32	0.35	14
Betz ratio					
Body weight	0.25	0.18–0.31	0.21	0.73	25
Brain weight	0.30	0.23–0.37	0.26	0.77	25
Neocortex volume	0.26	0.19–0.33	0.23	0.79	17
EQ	0.77	0.20–1.35	0.39	0.25	25
Meynert ratio					
Body weight	0.07	0.01–0.14	0.03	0.21	21
Brain weight	0.09	0.01–0.16	0.04	0.22	21
Neocortex volume	0.08	0.00–0.15	0.04	0.24	16
EQ	0.23	–0.13–0.58	0.07	0.08	21

brain and body size variables predicted specialized pyramidal cell soma volumes better than neighboring pyramidal cell soma volumes (table 2). The regression slopes of all neuron subtypes, except Betz cells, were statistically indistinguishable. Thus, increases in brain and body size had disproportionate effects on Betz soma volumes in comparison to layer V motor pyramidal neuron soma volumes, such that Betz soma volumes were relatively larger in bigger primate brains and bodies. Meynert somata and visual pyramidal cell somata, by contrast, scaled against brain and body size variables with statistically similar slopes, signifying a relatively constant relationship between pyramidal cell soma volume and Meynert soma volume. On average, Meynert somata were 2.8 times larger than visual pyramidal cell somata.

Due to the differential scaling of Betz somata in relation to brain size, the largest Betz ratios were found among the large-brained hominoids and Old World monkeys, with humans having the largest value (table 3). The patas monkey *(Erythrocebus patas)* was unusual in having a larger Betz ratio than any of the great apes although its brain is four times smaller. The terrestrial Old World monkeys *(Erythrocebus patas, Papio anubis,* and *Papio cynocephalus)* had the largest Meynert ratios of all species examined. Betz ratios were significantly correlated with body weight ($r = 0.67$, $p < 0.001$, $n = 25$), brain weight ($r = 0.78$, $p < 0.001$, $n = 25$), neocortical volume ($r = 0.79$, $p < 0.001$, $n = 18$), and EQ ($r = 0.56$, $p = 0.004$, $n = 25$) (fig. 5). Meynert ratios, however, were not correlated with any brain or body size variables (fig. 6).

Table 3. Species rank order of Betz and Meynert ratios

Species	Betz ratio	Species	Meynert ratio
Homo sapiens	10.96	*Erythrocebus patas*	5.80
Erythrocebus patas	8.86	*Papio anubis*	4.86
Gorilla gorilla	8.37	*Papio cynocephalus*	4.10
Papio cynocephalus	8.06	*Pan troglodytes*	3.78
Pan troglodytes	7.02	*Daubentonia madagascariensis*	3.15
Papio anubis	6.90	*Alouatta seniculus*	3.05
Pongo pygmaeus	6.51	*Gorilla gorilla*	2.98
Macaca nigra	5.34	*Aotus trivirgatus*	2.88
Alouatta seniculus	4.76	*Homo sapiens*	2.84
Macaca fuscata	4.27	*Saguinus mystax*	2.73
Perodicticus potto	3.73	*Macaca fascicularis*	2.66
Lemur catta	3.66	*Otolemur crassicaudatus*	2.43
Macaca fascicularis	3.56	*Perodicticus potto*	2.42
Pteropus poliocephalus	3.17	*Hapalemur griseus*	2.41
Daubentonia madagascariensis	3.10	*Tarsius syrichta*	2.24
Lagothrix lagotricha	2.80	*Propithecus verreauxi*	2.23
Aotus trivirgatus	2.71	*Loris tardigradus*	2.15
Tarsius syrichta	2.70	*Lagothrix lagotricha*	2.12
Propithecus verreauxi	2.52	*Pteropus poliocephalus*	2.11
Saguinus mystax	2.44	*Pongo pygmaeus*	1.94
Loris tardigradus	2.06	*Tupaia glis*	1.93
Galago senegalensis	2.05	*Lemur catta*	1.71
Hapalemur griseus	1.97		
Otolemur crassicaudatus	1.58		
Tupaia glis	1.58		

We determined the best predictors of Betz and Meynert ratios with stepwise multiple regression. Brain weight, body weight, EQ, and social group size were entered as predictors. The best model for Betz ratio included only brain weight as a predictor and explained a substantial amount of the variance ($t = 6.22$, $p < 0.001$, $R^2 = 0.67$). The best model for Meynert ratio included only group size as a predictor and explained a moderate amount of variance ($t = 2.22$, $p = 0.041$, $R^2 = 0.23$). Meynert ratios were compared among diet and habitat categories by one-way ANOVA. Although Meynert ratio did not show significant differences among dietary categories, there were significant differences between habitat categories. Meynert ratios were significantly larger among terrestrial anthropoids ($F = 10.75$, $p = 0.008$, d.f. = 11), but there was no effect among prosimians.

Because Betz ratio was correlated with brain weight, Betz ratios were compared among diet and habitat categories using analysis of covariance (ANCOVA) with brain weight as a covariate. Betz ratios were significantly larger among terrestrial anthropoids ($F = 40.86$, $p < 0.001$, d.f. = 13), but not among prosimians and there was no effect of dietary category.

Although there was a general trend for increasing Betz ratios in relation to brain weight, several individual species fell outside the limits of the 95% CI of the regression line (fig. 5). In particular, Betz ratios were larger than predicted in *Tarsius syrichta* (+37%), *Pteropus poliocephalus* (+31%), *Erythrocebus patas* (+26%), *Perodicticus potto* (+24%), and *Papio cynocephalus* (+16%). Betz ratios were relatively low in *Otolemur crassicaudatus* (–107%), *Lagothrix lagothricha* (–54%), *Hapalemur griseus* (–49%), *Propithecus verreauxi* (–29%), and *Tupaia glis* (–22%). Assuming that the Betz cells we sampled represent the forelimb, we hypothesized that disproportionate Betz ratios might be related to digital dexterity. To test this idea we performed a correlation analysis using a comparative index of digital dexterity [Heffner and Masterton, 1983] and the residuals from the regression of Betz ratio on brain size variables. In the small sample available, Betz ratio residuals and digital dexterity were not correlated.

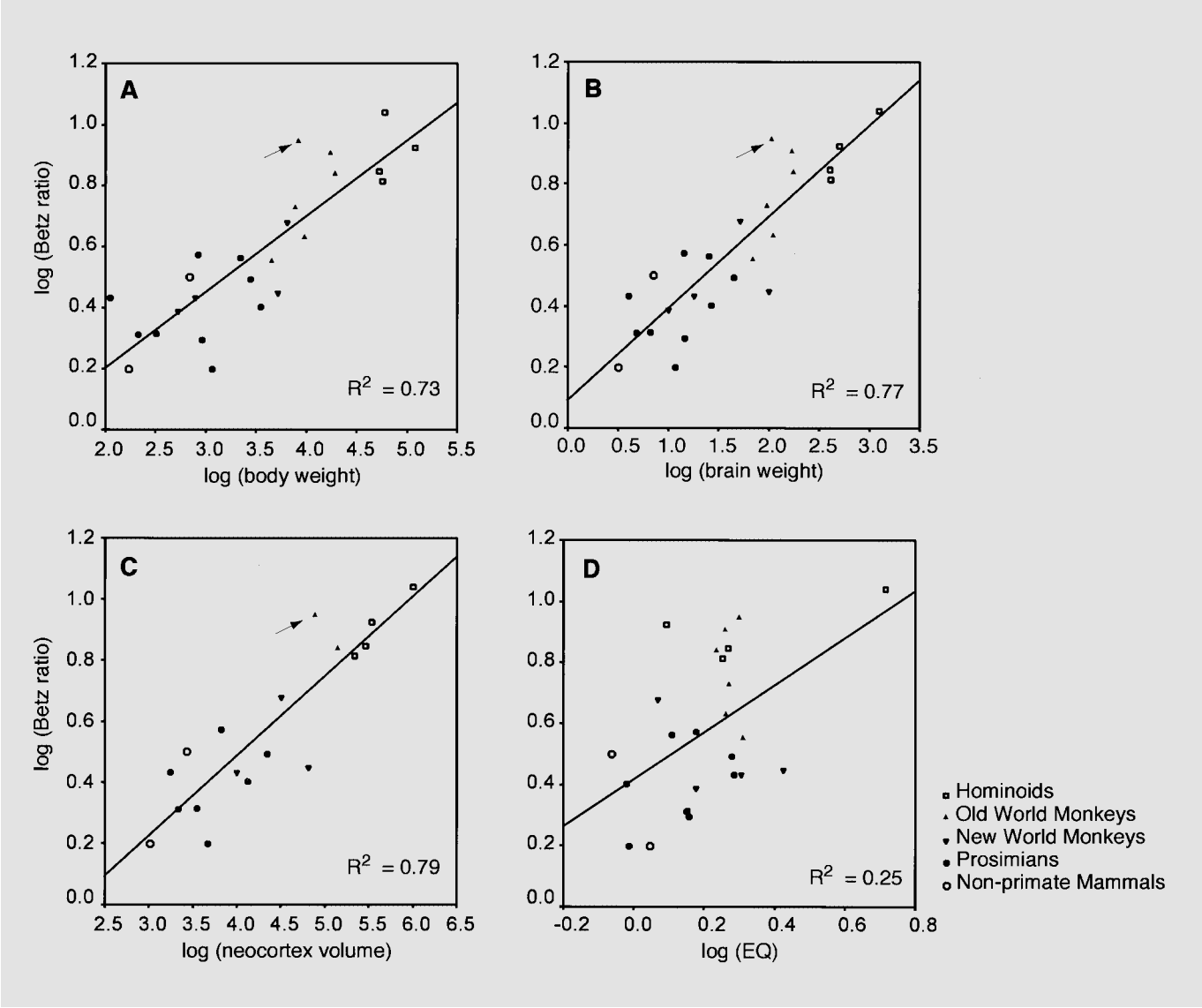

Fig. 5. Least-squares regression plots of Betz ratio against body weight (A), brain weight (B), neocortex volume (C), and EQ (D). Betz ratio is significantly correlated with body weight, brain weight, and neocortex volume (A–C). The patas monkey (indicated by arrows in A–C) has a relatively large Betz ratio, possibly due to its locomotor adaptation to an open savannah habitat.

Discussion

Neuronal soma volume is determined by the biosynthetic and metabolic requirements of the entire cell, including its dendritic arbors and axon [Kaas, 2000]. Therefore, evolutionary enlargement of Betz and Meynert somata represent increases in the thickness and/or ramifications of these cells' neurites. Although the high metabolic demands of brain tissue and wiring constraints on connected systems act as strong selective pressures to reduce neuron size and minimize the space occupied by neurites [Aiello and Wheeler, 1995; Chklovskii et al., 2002], the emergence of the gigantopyramidal Betz and Meynert subtypes, in spite of these constraints, attests to their special significance in adaptive sensorimotor function of primates.

Our data show that Betz and Meynert cell somata adhere to different scaling rules which could be inter-

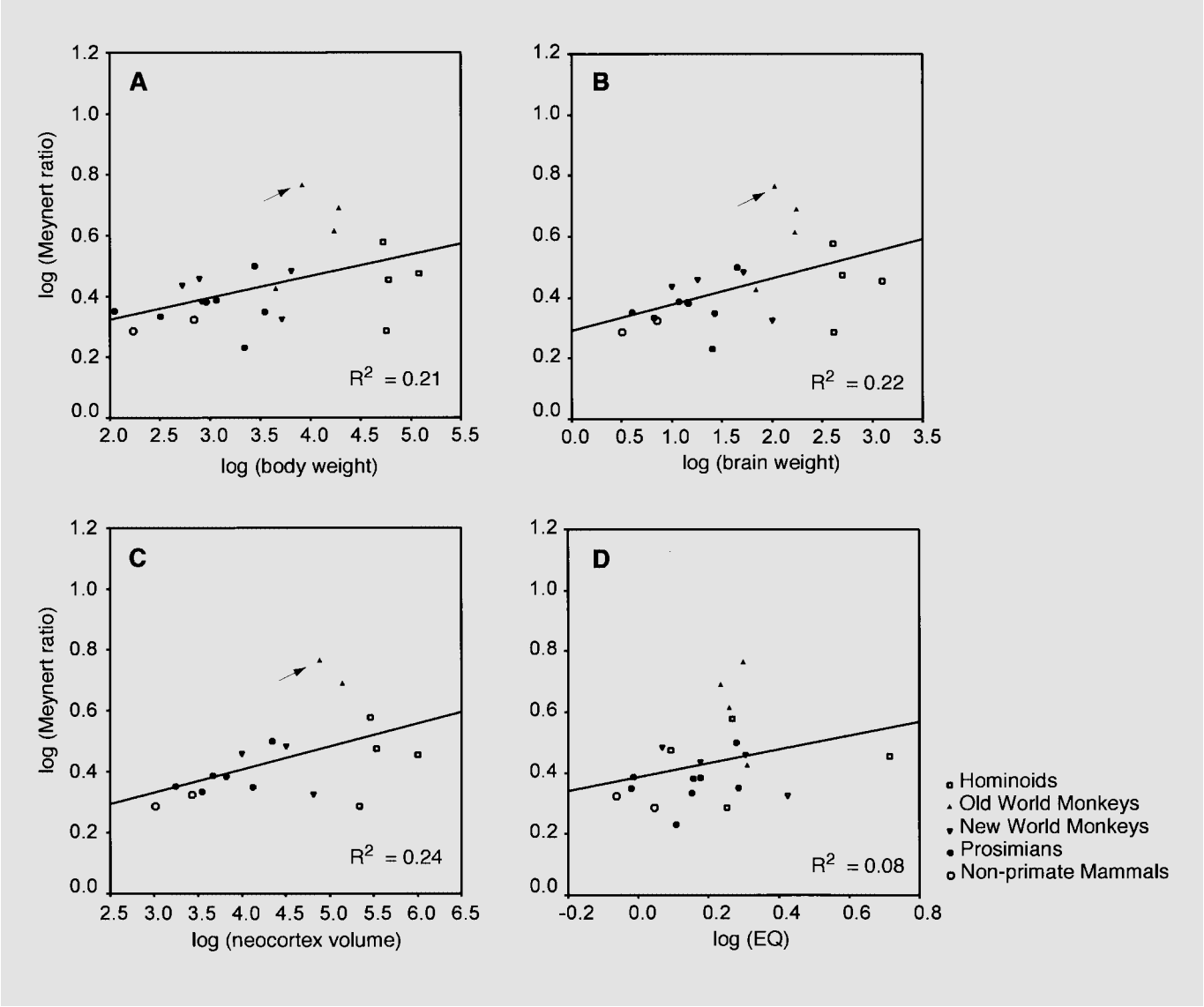

Fig. 6. Least-squares regression plots of Meynert ratio against body weight (A), brain weight (B), neocortex volume (C), and EQ (D). Meynert ratio is not correlated with any brain or body size variable. The patas monkey (indicated by arrows in A–C) has a relatively large Meynert ratio, possibly due to its function in predator detection in an open savannah habitat.

preted in the context of their different functional anatomical roles. Before discussing these results, however, a few methodological limitations of the present study should be mentioned. The tissue used in many cases derived from rare species which were represented by small samples. Also, archival slide collections were used for several species and, therefore, sex and exact age could not be determined in a significant portion of the sample. Available evidence, however, indicates that cortical neuronal soma sizes do not differ between human males and females [Rabinowicz et al., 2002]. Finally, due to the opportunistic availability of specimens, analyses of scaling used brain weights and body weights reported in the literature rather than from the same individuals in which cellular volumes were measured.

Cellular volumes of all infragranular pyramidal neuron subtypes were negatively allometric with respect to brain and body size variables. To maintain rapid impulse con-

duction and reduce the space occupied by wires at larger brain sizes, neurons are connected in local networks [Deacon, 1990; Ringo, 1991] such that evolutionary enlargement of neocortex is accomplished by the addition of cortical columns, rather than by the expansion of them [Rakic, 1995]. Indeed, cortical columns are relatively invariant in their horizontal extent compared to the extreme interspecific variability in the surface area of cortex [Mountcastle, 1998; Buxhoeveden and Casanova, 2002]. This emphasis on short-range connections leads to cellular volumes that increase more slowly than total brain size [Haug, 1987]. The scaling differences between Betz cells and Meynert cells, however, might be related to fundamental differences in the local network allometry of motor and visual cortices.

Although primary motor cortex (area 4) is somatotopically organized [Leyton and Sherrington, 1917; Bucy, 1949; Penfield and Rasmussen, 1950; Woolsey et al., 1952], cortical modules in area 4 do not simply represent individual muscles or motor units [Schieber, 2001]. Each muscle is represented multiple times over a wide region. Cortical modules in area 4 represent movement direction and force across a joint with pyramidal neurons making synapses on motoneurons that innervate several different muscles [Mountcastle, 1998]. Thus, modules in area 4 have complex horizontal interconnections across large spans of cortex to coordinate movements [Huntley and Jones, 1991; Baker et al., 1998]. Our results show that Betz somata in the region of hand representation become relatively enlarged with increases in brain and body size. At larger sizes, there is an increase in the distance to the spinal representation of target muscles and a greater number of less densely distributed corticospinal neurons [Nudo et al., 1995]. Betz cells produce rapid bursts of early activity to set supportive muscle tone prior to the implementation of a specific motor program [Evarts, 1965] and have basal dendrites that form bundles with the dendrites of neighboring infragranular neurons and might influence their threshold level of excitability through changes in local electrical and chemical gradients [Scheibel and Scheibel, 1978]. To conserve this function in the context of larger brains and bodies, Betz cell axons might become thicker to boost conduction speed and extend their dendritic field to preserve connections with a more dispersed population of cortical modules.

We did not find a relationship between Betz ratio residuals and digital dexterity. This result is unlikely due to difficulties in accurately identifying the region of forelimb representation. In a study of humans, we found that within and surrounding the region of hand representation covering approximately 6 cm, Betz ratios do not vary significantly [Rivara et al., 2003]. Indeed, it is not surprising that a correlation does not exist between Betz cell size and digital dexterity because, unlike smaller projection neurons, Betz cells control alpha motoneurons without access to direct sensory feedback making it unlikely that they participate in the refinement of precise dexterous movements [Marsden et al., 1984; Zilles, 1990]. Enlarged Betz somata, however, might serve a role in some aspects of locomotor adaptation of primates. Relatively large Betz ratios, for example, were found in patas monkeys who employ extremely rapid digitigrade quadrupedal locomotion [Gebo and Sargis, 1994], and pottos who are slow arboreal quadruped climbers with especially strong grasping hands and feet [Fleagle, 1999].

Primary visual cortex (area 17) consists of a mosaic of iterated overlapping modules that each process different input features from a local region of visual space. Fundamentally, modules in area 17 form a two-dimensional topographic map of retinal input with strong interconnections between adjacent modules [Rockland and Lund, 1983]. As such, visual neurons are scaled to local rather than global connectivity demands. For example, the horizontal connections of tree shrew [Lyon et al., 1998] and macaque [Rockland and Lund, 1983] visual neurons extend over a similar distance although area 17 of macaques is considerably larger. Meynert cells are positioned in the context of these local processing modules; in anthropoids the long-axis of Meynert cell basal dendrites is oriented parallel to individual ocular dominance columns [Neal et al., 1985] and Meynert somata are arranged underneath voids in the complex of cytochrome oxidase active color-sensitive patches in layers II and III [Payne and Peters, 1989]. The parallel scaling of Meynert somata and neighboring visual pyramidal cell somata might be due to the fact that, although Meynert cell axons must project more distantly to the temporal lobe and midbrain in larger brains, the size of their dendritic field is largely constrained by their function in a local circuit that is rather invariant in size.

According to our analysis, some of the variance in Meynert ratio can be explained by social group size and habitat. It has been suggested that terrestrial anthropoids living in open savannah and semi-desert habitats are more susceptible to predation and large group size could be, in part, a response to increased predation pressure [van Schaik et al., 1983; Janson, 1992]. Although predation-related mortality rates are difficult to estimate as these events are rarely observed directly by primatologists, the ubiquity and specificity of predator alarm calls

among terrestrial anthropoids suggests that these species are particularly vigilant of predator movements [Seyfarth et al., 1980]. We speculate that part of the neural basis of predator vigilance involves relatively large Meynert somata possessing dendritic fields that extend across a large number of orientation and ocular dominance columns that are capable of integrating input from greater expanses of visual space. Importantly, our data, taken together with recent evidence that human area 17 has a novel mesh-like geometric arrangement of magnocellular-related dendrites in layer IVA [Preuss et al., 1999; Preuss and Coleman, 2002], highlights the possibility that cortical specializations of the motion-processing pathway of primates might occur in the absence of dramatic changes in encephalization or the volume of area 17.

Finally, the enlargement and differentiation of Betz and Meynert cells can be viewed as a correlate of the specialization of functionally distinct regions of the neocortex in primates. In this context, it is interesting that another unique cell class, a large spindle cell, has been found in the anterior cingulate and insular cortices of only great apes and humans [Nimchinsky et al., 1999]. In humans, these spindle cells are highly vulnerable to neurodegeneration in Alzheimer's disease, further emphasizing the importance of comparative studies in the context of aging and age-related diseases [Nimchinsky et al., 1995, 1999]. Whereas few changes to Betz and Meynert cells have been reported in Old World monkeys during aging [Tigges et al., 1992; Hof et al., 2000, 2002; Hof and Duan, 2001], there is evidence that Meynert cells are affected in Alzheimer's disease [Hof and Morrison, 1990] and Betz cells in amyotrophic lateral sclerosis [Sasaki and Iwata, 2000] and normal aging in humans [Scheibel et al., 1977]. Betz cells in elderly humans exhibit dendritic attrition and somatic swelling. Additional studies will be needed to evaluate the effects of aging on these specialized neuron subtypes in great apes to determine the evolutionary onset of human-like neuropathological aging.

Acknowledgements

We thank Drs. E.A. Nimchinsky and P.J. Gannon, and E.C. Kirk, E. Bush, and S.C. McFarlin for helpful discussion, Drs. K. Zilles and H.D. Frahm for help with the Stephan collection, and C. Buitron and V.V. Oruganti for expert technical assistance. Great ape specimens used in this study were on loan to the Comparative Neurobiology of Aging Resource supported by NIH AG14308. This work was supported by the Leakey Foundation, the Wenner-Gren Foundation, NSF BCS0121286, NSF DBI9602234 (to NYCEP), and the Mount Sinai School of Medicine. P.R. Hof is the Regenstreif Professor of Neuroscience.

References

Aiello, L.C., and P. Wheeler (1995) The expensive-tissue hypothesis: the brain and the digestive system in human and primate evolution. Curr. Anthropol., *36:* 199–211.

Allman, J.M., and J.H. Kaas (1971) Representation of the visual field in striate and adjoining cortex of the owl monkey *(Aotus trivirgatus)*. Brain Res., *35:* 89–106.

Allman, J.M. (1999) Evolving Brains. Scientific American Library, New York.

Baker, S.N., E. Olivier, and R.N. Lemon (1998) An investigation of the intrinsic circuitry of the motor cortex of the monkey using intra-cortical microstimulation. Exp. Brain Res., *123:* 397–411.

Baron, G., H. Stephan, and H.D. Frahm (1996) Comparative Neurobiology in Chiroptera. Birkhäuser Verlag, Basel.

Betz, W. (1874) Anatomischer Nachweis Gehirncentra. Zbl. med. Wiss., *12:* 578–580, 594–599.

Betz, W. (1881) Über die feineren Strukturen der Gehirnrinde des Menschen. Zbl. med. Wiss., *19:* 193–195, 210–213, 231–234.

Boroojerdi, B., H. Foltys, T. Krings, U. Spetzger, A. Thron, and R. Topper (1999) Localization of the motor hand area using transcranial magnetic stimulation and functional magnetic resonance imaging. Clin. Neurophysiol., *110:* 699–704.

Braak, H., and E. Braak (1976) The pyramidal cells of Betz within the cingulate and precentral gigantopyramidal field in the human brain. A Golgi and pigmentarchitectonic study. Cell Tissue Res., *172:* 103–119.

Brodmann, K. (1903) Beiträge zur histologischen Lokalisation der Grosshirnrinde. 1. Mitteilung: die Regio rolandica. J. Psychol. Neurol., *2:* 79–107.

Brodmann, K. (1909) Vergleichende Lokalisationslehre der Grosshirnrinde in ihren Prinzipien auf Grund des Zellenbaues. Barth, Leipzig.

Bucy, P.C. (1949) Effects of extirpation in man. *In* The Precentral Motor Cortex (ed. by P.C. Bucy), University of Illinois Press, Urbana, pp. 353–394.

Buxhoeveden, D.P., and M.F. Casanova (2002) The minicolumn hypothesis in neuroscience. Brain, *125:* 935–951.

Campbell, A.W. (1905) Histological Studies on the Localization of Cerebral Function. Cambridge University Press, London, UK.

Chan-Palay, V., S.L. Palay, and S.M. Billings-Gagliardi (1974) Meynert cells in the primate visual cortex. J. Neurocytol., *3:* 631–658.

Chklovskii, D.B., T. Schikorski, and C.F. Stevens (2002) Wiring optimization in cortical circuits. Neuron, *34:* 341–347.

Clutton-Brock, T.H., and P.H. Harvey (1980) Primates, brains, and ecology. J. Zool. Lond., *190:* 309–323.

Craggs, M.D., D.N. Rushton, and D.G. Clayton (1976) The stability of the electrical stimulation map of the motor cortex of the anesthetized baboon. Brain., *99:* 575–600.

Deacon, T.W. (1990) Fallacies of progression in theories of brain-size evolution. Int. J. Primatol., *11:* 193–235.

DeBruyn, E.J., V.A. Casagrande, P.D. Beck, and A.B. Bonds (1993) Visual resolution and sensitivity of single cells in the primary visual cortex (V1) of a nocturnal primate (bush baby): correlations with cortical layers and cytochrome oxidase patterns. J. Neurophysiol., *69:* 3–18.

Donoghue, J.P., S. Leibovic, and J.N. Sanes (1992) Organization of the forelimb area in squirrel monkey motor cortex: representation of digit, wrist, and elbow muscles. Exp. Brain Res., *89:* 1–19

Dunbar, R.I.M. (1992) Neocortex size as a constraint on group size in primates. J. Hum. Evol., *20:* 469–493.

Dusser de Barenne, J.G., H.W. Garol, and W.S. McCulloch (1941) The 'motor' cortex of the chimpanzee. J. Neurophysiol., *4:* 287–304.

Evarts, E.V. (1965) Relation of discharge frequency to conduction velocity in pyramidal tract neurons. J. Neurophysiol., *28:* 216–228.

Flaherty, A.W., and A.M. Graybiel (1995) Motor and somatosensory corticostriatal projection magnifications in the squirrel monkey. J. Neurophysiol., *74:* 2638–2648.

Fleagle, J.G. (1999) Primate Adaptation and Evolution. Academic Press, San Diego.

Fogassi, L., V. Gallese, M. Gentilucci, G. Luppino, M. Matelli, and G. Rizzolatti (1994) The fronto-parietal cortex of the prosimian Galago: patterns of cytochrome oxidase activity and motor maps. Behav. Brain Res., *60:* 91–113.

Fries, W., and H. Distel (1983) Large layer VI neurons of monkey striate cortex (Meynert cells) project to the superior colliculus. Proc. R. Soc. Lond. B Biol. Sci., *219:* 53–59.

Fries, W., K. Keizer, and H.G. Kuypers (1985) Large layer VI cells in macaque striate cortex (Meynert cells) project to both superior colliculus and prestriate visual area V5. Exp. Brain Res., *58:* 613–616.

Fries, W. (1986) Distribution of Meynert cells in primate striate cortex. Spatial relationships with cytochrome oxidase blobs. Naturwissenschaften, *73:* 557–558.

Galaburda, A.M., D.P. Holinger, U. Bellugi, and G.F. Sherman (2002) Williams syndrome: neuronal size and neuronal-packing density in primary visual cortex. Arch. Neurol., *59:* 1461–1467.

Gebo, D.L., and E.J. Sargis (1994) Terrestrial adaptations in the postcranial skeletons of guenons. Am. J. Phys. Anthropol., *93:* 341–371.

Gould, H.J., C.G. Cusick, T.P. Pons, and J.H. Kaas (1986) The relationship of corpus callosum connections to electrical stimulation maps of motor, supplementary motor, and the frontal eye fields in owl monkeys. J. Comp. Neurol., *247:* 297–325.

Groves, C. (2001) Primate Taxonomy. Smithsonian Institute Press, Washington.

Grünbaum, A.S.F., and C.S. Sherrington (1903–04) Observations on the physiology of the cerebral cortex of the anthropoid apes. Proc. R. Soc., *72:* 152–155.

Harvey, P.H., R.D. Martin, and T.H. Clutton-Brock (1987) Life histories in comparative perspective. *In* Primate Societies (ed. by B.B. Smuts, D.L. Cheney, R.M. Seyfarth, R.W. Wrangham and T.T. Strusaker), University of Chicago Press, Chicago, pp. 181–196.

Haug, R. (1987) Brain sizes, surfaces, and neuronal sizes of the cortex cerebri: A stereological investigation of man and his variability and a comparison with some mammals (primates, whales, marsupials, insectivores, and one elephant). Am. J. Anat., *180:* 126–142.

Hayes, T.L., and D.A. Lewis (1995) Anatomical specialization of the anterior motor speech area: hemispheric differences in magnopyramidal neurons. Brain Lang., *49:* 289–308.

Heffner, R.S., and R.B. Masterton (1983) The role of the corticospinal tract in the evolution of human digital dexterity. Brain. Behav. Evol., *23:* 165–183.

Hines, M. (1940) Movements elicited from the precentral gyrus of adult chimpanzees by stimulation with sine wave currents. J. Neurophysiol., *3:* 442–466.

Hlustik, P., A. Solodkin, R.P. Gullapalli, D.C. Noll, and S.L. Small (2001) Somatotopy in human primary motor cortex and somatosensory hand representations revisited. Cereb. Cortex., *11:* 312–321.

Hof, P.R., and H. Duan (2001) Age-related morphologic alterations in the brain of Old World and New World anthropoid monkeys. *In* Functional Neurobiology of Aging (ed. by P.R. Hof and C.V. Mobbs), Academic Press, San Diego, pp. 435–446.

Hof, P.R., and J.H. Morrison (1990) Quantitative analysis of a vulnerable subset of pyramidal neurons in Alzheimer's disease: II. Primary and secondary visual cortex. J. Comp. Neurol., *301:* 55–64.

Hof, P.R., and J.H. Morrison (1995) Neurofilament protein defines regional patterns of cortical organization in the macaque monkey visual system: a quantitative immunohistochemical analysis. J. Comp. Neurol., *352:* 161–186.

Hof, P.R., E.P. Gilissen, C.C. Sherwood, H. Duan, P.W.H. Lee, B.D. Delman, T.P. Naidich, P.J. Gannon, D.P. Perl, and J.M. Erwin (2002) Comparative neuropathology of brain aging in primates. *In* Aging in Nonhuman Primates (ed. by J.M. Erwin and P.R. Hof), Karger, Basel, pp. 130–154.

Hof, P.R., E.A. Nimchinsky, W.G. Young, and J.H. Morrison (2000) Numbers of Meynert and layer IVB cells in area V1: a stereologic analysis in young and aged macaque monkeys. J. Comp. Neurol., *420:* 113–126.

Holloway, R.L. (1996) Toward a synthetic theory of human brain evolution. *In* Origins of the Human Brain (ed. by J.P. Changeux and J. Chavaillon), Clarendon Press, Oxford, UK, pp. 42–54.

Humphrey, D.R. (1986) Representation of movements and muscles within the primate precentral motor cortex: historical and current perspectives. Federation Proc., *45:* 2687–2699.

Huntley, G.W., and E.G. Jones (1991) Relationship of intrinsic connections of forelimb movement representations in monkey motor cortex: A correlative anatomical and physiological study. J. Neurophysiol., *66:* 390–413.

Janson, C.H. (1992) Evolutionary ecology of primate social structure. *In* Evolutionary Ecology and Human Behaviour (ed. by E.A. Smith and B. Winterhalder), Aldine, New York, pp. 95–130.

Kaas, J.H. (2000) Why is brain size so important: design problems and solutions as neocortex gets bigger or smaller. Brain Mind, *1:* 7–23.

Kaas, J.H., W.C. Hall, H. Killackey, and I.T. Diamond (1972) Visual cortex of the tree shrew *(Tupaia glis)*: Architectonic subdivisions and representation of the visual field. Brain Res., *42:* 491–496.

Kretz, R., G. Rager, and T.T. Norton (1986) Laminar organization of ON and OFF regions and ocular dominance in the striate cortex of the tree shrew *(Tupaia belangeri)*. J. Comp. Neurol., *251:* 135–145.

Krubitzer, L.A., and J.H. Kaas (1990) The organization and connections of somatosensory cortex in marmosets. J. Neurosci., *10:* 952–974.

Krubitzer, L., J.C. Clarey, R. Tweedale, and M.B. Calford (1998) Interhemispheric connections of somatosensory cortex in the flying fox. J. Comp. Neurol., *402:* 538–559.

Kwan, H.C., W.A. MacKay, J.T. Murphy, and Y.C. Wong (1978) Spatial organization of precentral cortex in awake primates. II. Motor outputs. J. Neurophysiol., *41:* 1120–1131.

Lassek, A.M. (1948) The pyramidal tract: Basic considerations of corticospinal neurons. Ass. Res. Nerv. Ment. Dis., *27:* 106–128.

Le Gros Clark, W.E. (1942) The cells of Meynert in the visual cortex of the monkey. J. Anat., *74:* 369–376.

Le Gros Clark, W.E. (1959) The Antecedents of Man. Edinburgh University Press, Edinburgh.

Leyton, A.S.F., and C.S. Sherrington (1917) Observations on the excitable cortex of the chimpanzee, orang-utan, and gorilla. Q. J. Exp. Physiol., *11:* 137–222.

Livingstone, M.S. (1998) Mechanisms of direction selectivity in macaque V1. Neuron, *20:* 509–526.

Lund, J.S., R.D. Lund, A.E. Hendrickson, A.H. Bunt, and A.F. Fuchs (1975) The origin of efferent pathways from the primary visual cortex, area 17, of the macaque monkey as shown by retrograde transport of horseradish peroxidase. J. Comp. Neurol., *164:* 287–303.

Lyon, D.C., N. Jain, and J.H. Kaas (1998) Cortical connections of striate and extrastriate visual areas in tree shrews. J. Comp. Neurol., *401:* 109–128.

Marsden, C.D., J.C. Rothwell, and B.L. Day (1984) The use of peripheral feedback in the control of movement. Trends Neurosci., *7:* 253–257.

Martin, R.D. (1981) Relative brain size and basal metabolic rate in terrestrial vertebrates. Nature, *293:* 57–60.

Martin, R.D. (1990) Primate Origins and Evolution. Princeton University Press, Princeton.

Meyer, G. (1987) Forms and spatial arrangement of neurons in the primary motor cortex of man. J. Comp. Neurol., *262:* 402–428.

Meynert, T. (1867) Der Bau der Grosshirnrinde und seine örtlichen Verschiedenheiten nebst einem pathologisch anatomischen Corollarium. Vjschr. Psychiat., *1:* 198–217.

Mountcastle, V.B. (1998) Perceptual Neuroscience: The Cerebral Cortex. Harvard University Press, Cambridge.

Movshon, J.A., and W.T. Newsome (1996) Visual response properties of striate cortical neurons projecting to area MT in macaque monkeys. J. Neurosci., *16:* 7733–7741.

Neal, J.W., D.A. Winfield, and T.P. Powell (1985) The effect of visual deprivation upon the basal dendrites of Meynert cells in the striate cortex of the monkey. Proc. R. Soc. Lond. B Biol. Sci., *225:* 411–423.

Newsome, W.T., and J.M. Allman (1980) Interhemispheric connections of visual cortex in the owl monkey, *Aotus trivirgatus*, and the bush baby, *Galago senegalensis*. J. Comp. Neurol., *194:* 209–233.

Nimchinsky, E.A., E. Gilissen, J.M. Allman, D.P. Perl, J.M. Erwin, and P.R. Hof (1999) A neuronal morphologic type unique to humans and great apes. Proc. Natl. Acad. Sci. USA, *96:* 5268–5273.

Nimchinsky, E.A., B.A. Vogt, J.H. Morrison, and P.R. Hof (1995) Spindle neurons of the human anterior cingulate cortex. J. Comp. Neurol., *355:* 27–37.

Nimchinsky, E.A., W. Young, G. Yeung, R.A. Shah, J.W. Gordon, F.E. Bloom, J.H. Morrison, and P.R. Hof (2000) Differential vulnerability of oculomotor, facial and hypoglossal nuclei in G86R superoxide dismutase transgenic mice. J. Comp. Neurol., *416:* 112–125.

Nudo, R.J., D.P. Sutherland, and R.B. Masterton (1995) Variation and evolution of mammalian corticospinal somata with special reference to primates. J. Comp. Neurol., *358:* 181–205.

Palay, S.L. (1978) The Meynert cell, an unusal cortical pyramidal cell. *In* Architectonics of the Cerebral Cortex (ed. by M.A.B. Brazier and H. Petsche), Raven Press, New York, pp. 31–42.

Park, M.C., A. Belhaj-Saif, M. Gordon, and P.D. Cheney (2001) Consistent features in the forelimb representation of primary motor cortex in rhesus macaques. J. Neurosci., *21:* 2784–2792.

Payne, B.R., and A. Peters (1989) Cytochrome oxidase patches and Meynert cells in monkey visual cortex. Neuroscience, *28:* 353–363.

Penfield, W., and T. Boldrey (1937) Somatic motor and sensory representation in the cerebral cortex of man as studied by electrical stimulation. Brain, *37:* 389–443.

Penfield, W., and T. Rasmussen (1950) The Cerebral Cortex of Man: A Clinical Study of Localization of Function. Macmillan, New York.

Preuss, T.M., and G.Q. Coleman (2002) Human-specific organization of primary visual cortex: alternating compartments of dense Cat-301 and calbindin immunoreactivity in layer 4A. Cereb. Cortex, *12:* 671–691.

Preuss, T.M., P.D. Beck, and J.H. Kaas (1993) Areal, modular, and connectional organization of visual cortex in a prosimian primate, the slow loris *(Nycticebus coucang)*. Brain Behav. Evol., *42:* 321–335.

Preuss, T.M., I. Stepniewska, and J.H. Kaas (1996) Movement representation in the dorsal and ventral premotor areas of owl monkeys: a microstimulation study. J. Comp. Neurol., *371:* 649–676.

Preuss, T.M., H. Qi, and J.H. Kaas (1999) Distinctive compartmental organization of human primary visual cortex. Proc. Natl. Acad. Sci. USA, *96:* 11601–11606.

Rabinowicz, T., J.M. Petetot, P.S. Gartside, D. Sheyn, and T.de C.M. Sheyn (2002) Structure of the cerebral cortex in men and women. J. Neuropathol. Exp. Neurol., *61:* 46–57.

Rakic, P. (1995) A small step for the cell, a giant leap for mankind: a hypothesis of neocortical expansion during evolution. Trends Neurosci., *18:* 383–388.

Ramón y Cajal, S. (1899) Estudios sobre la corteza cerebral humana. Corteza visual. Rev. Trim. Microgr., *4:* 1–63.

Ringo, J.L. (1991) Neuronal interconnection as a function of brain size. Brain Behav. Evol., *38:* 1–6.

Rivara, C.-B., C.C. Sherwood, C. Bouras, and P.R. Hof (2003) Stereologic characterization and spatial distribution patterns of Betz cells in human primary motor cortex. Anat. Rec., *270A:* 137–151.

Rockland, K.S., and T. Knutson (2001) Axon collaterals of Meynert cells diverge over large portions of area V1 in the macaque monkey. J. Comp. Neurol., *441:* 134–147.

Rockland, K.S., and J.S. Lund (1983) Intrinsic laminar lattice connections in primate visual cortex. J. Comp. Neurol., *216:* 303–318.

Rosa, M.G., K.A. Fritsches, and G.N. Elston (1997) The second visual area in the marmoset monkey: visuotopic organisation, magnification factors, architectonical boundaries, and modularity. J. Comp. Neurol., *387:* 547–567.

Rosa, M.G., L.M. Schmid, L.A. Krubitzer, and J.D. Pettigrew (1993) Retinotopic organization of the primary visual cortex of flying foxes *(Pteropus poliocephalus* and *Pteropus scapulatus)*. J. Comp. Neurol., *335:* 55–72.

Rowe, N. (1996) The Pictorial Guide to the Living Primates. Pogonias Press, East Hampton, NY.

Samulack, D.D., R.S. Waters, R.W. Dykes, and P.A. McKinley (1990) Absence of responses to microstimulation at the hand-face border in baboon primary motor cortex. Can. J. Neurol. Sci., *17:* 24–29.

Sasaki, S., and M. Iwata (2000) Immunocytochemical and ultrastructural study of the motor cortex in patients with lower motor neuron disease. Neurosci. Lett., *281:* 45–48.

Sato, K.C., and J. Tanji (1989) Digit-muscle responses evoked from multiple intracortical foci in monkey precentral motor cortex. J. Neurophysiol., *62:* 959–970.

Scheibel, M.E., and A.B. Scheibel (1978) The dendritic structure of the human Betz cell. *In* Architectonics of the Cerebral Cortex (ed. by M.A.B. Brazier and H. Pets), Raven Press, New York, pp. 43–57.

Scheibel, M.E., U. Tomiyasu, and A.B. Scheibel (1977) The aging human Betz cell. Exp. Neurol., *56:* 598–609.

Schieber, M.H. (2001) Constraints on somatotopic organization in the primary motor cortex. J. Neurophysiol., *86:* 2125–2143.

Schmitz, C., D. Schuster, P. Niessen, and H. Korr (1999) No difference between estimated mean nuclear volumes of various types of neurons in the mouse brain obtained on either isotropic uniform random sections or conventional frontal or sagittal sections. J. Neurosci. Methods, *88:* 71–82.

Seyfarth, R.M., D.L. Cheney, and P. Marler (1980) Monkey responses to three different alarm calls: evidence of predator classification and semantic communication. Science, *210:* 801–803.

Smith, R.J. (1999) Statistics of sexual dimorphism. J. Hum. Evol., *36:* 423–459.

Spatz, W.B. (1975) An efferent connection of the solitary cells of Meynert. A study with horseradish peroxidase in the marmoset *Callithrix*. Brain Res., *92:* 450–455.

Stephan, H., G. Baron, and H. Frahm (1988) Comparative size of brains and brain components. *In* Comparative Primate Biology: Neurosciences (ed. by H.D. Steklis and J. Erwin), Alan R. Liss, Inc., New York, pp. 1–38.

Stephan, H., H. Frahm, and G. Baron (1981) New and revised data on volumes of brain structures in Insectivores and Primates. Folia Primatol., *35:* 1–29.

Strick, P.L., and J.B. Preston (1978) Multiple representation in the primate motor cortex. Brain Res., *154:* 366–370.

Strick, P.L., and J.B. Preston (1982) Two representations of the hand in area 4 of a primate. I. Motor output organization. J. Neurophysiol., *48:* 139–149.

Tigges, J., J.G. Herndon, and A. Peters (1992) Axon terminals on Betz cell somata of area 4 in rhesus monkey throughout adulthood. Anat. Rec., *232:* 305–315.

Tigges, M., J. Tigges, and C.D. Sporborg (1981) Will the real Meynert cell please stand up? Soc. Neurosci. Abst., *7:* 831.

van Schaik, C.P., M.A. van Noordwijk, B. Warsono, and E. Sutriono (1983) Party size and early detection of predators in Sumatran forest primates. Primates, *24:* 211–221.

Vedel-Jensen, E.B., and H.J.G. Gundersen (1993) The rotator. J. Microsc., *170:* 35–44.

Vogt, C., and O. Vogt (1942) Morphologische Gestaltungen unter normalen und pathogenen Bedingungen. J. Psychol. Neurol., *50:* 524.

von Bonin, G. (1949) Architecture of the precentral motor cortex and some adjacent areas. *In* The Precentral Motor Cortex (ed. by P.C. Bucy), University of Illinois Press, Urbana, pp. 7–82.

von Bonin, G. (1950) The Isocortex of the Chimpanzee. University of Illinois Press, Urbana.

von Economo, C., and G.N. Koskinas (1925) Die Cytoarchitektonik der Hirnrinde des erwachsenen Menschen. Springer, Wein-Berlin.

Walshe, F.M. (1942) The giant cells of Betz, the motor cortex and the pyramidal tract: a critical review. Brain, *65:* 409–461.

Waters, R.S., D.D. Samulack, R.W. Dykes, and P.A. McKinley (1990) Topographic organization of baboon primary motor cortex: face, hand, forelimb, and shoulder representation. Somatosens. Mot. Res., *7:* 485–514.

Winfield, D.A., J.W. Neal, and T.P. Powell (1983) The basal dendrites of Meynert cells in the striate cortex of the monkey. Proc. R. Soc. Lond. B Biol. Sci., *217:* 129–139.

Winfield, D.A., M. Rivera-Dominguez, and T.P. Powell (1981) The number and distribution of Meynert cells in area 17 of the macaque monkey. Proc. R. Soc. Lond. B Biol. Sci., *213:* 27–40.

Woolsey, C.N., P.H. Settlage, D.R. Meyer, W. Sencer, T.P. Hamuy, and A.M. Travis (1952) Patterns of localization in precentral and 'supplementary' motor areas and their relation to the concept of a premotor area. Res. Pub. Assoc. Res. Nerv. Ment. Dis., *30:* 238–264.

Wu, C.W., N.P. Bichot, and J.H. Kaas (2000) Converging evidence from microstimulation, architecture, and connections for multiple motor areas in the frontal and cingulate cortex of prosimian primates. J. Comp. Neurol., *423:* 140–177.

Yousri, T.A., U.D. Schmid, H. Alkadhi, D. Schmidt, A. Peraud, A. Buettner, and P. Winkler (1997) Localization of the motor hand area to a knob on the precentral gyrus. A new landmark. Brain., *120:* 141–157.

Zeki, S. (1993) A Vision of the Brain. Blackwell Scientific, Oxford, UK.

Zilles, K. (1990) Cortex. *In* The Human Nervous System (ed. by G. Paxinos), Academic Press, San Diego, pp. 757–852.

Zilles, K., and G. Rehkämper (1988) The brain, with special reference to the telencephalon. *In* Orang-utan Biology (ed. by J.H. Schwartz), Oxford University Press, New York, pp. 157–176.

Zilles, K., H. Stephan, and A. Schleicher (1982) Quantitative cytoarchitectonics of the cerebral cortices of several prosimian species. *In* Primate Brain Evolution: Methods and Concepts (ed. by E. Armstrong and D. Falk), Plenum Press, New York, 177–202.